Ocean acoustic tomography: Travel-time inversion in the eastern Fram Strait

E. Skarsoulis[a], G. Piperakis[a], M. Kalogerakis[b] and H. Sagen[c]

[a]FORTH / IACM, N. Plastira 100, Vasilika Voutes, GR-70013 Heraklion, Greece
[b]TEI Crete / FORTH/IACM, Vassilika Vouton, GR-711 10 Heraklion, Crete, Greece
[c]Nansen Environmental and Remote Sensing Center, Thormølensgt. 47, 5006 Bergen, Norway
mixalis@iacm.forth.gr

An ocean acoustic tomography experiment in the framework of the DAMOCLES project is planned to be conducted in the eastern Fram Strait involving a 250-Hz acoustic source west of Spitzbergen and a vertical receiving array in the middle of the strait. This work focuses on methods developed for the analysis of travel - time data from the vertical receiving array. A discrete inversion scheme relying on the matched-peak approach will be applied to recover variations in the temperature distribution over the duration of the experiment. Data collected and transmitted from the experiment site will be handled and analyzed in near-real time by a dedicated software system.

1   Introduction

DAMOCLES (Developing Arctic Modeling and Observing Capabilities for Long-term Environmental Studies) is an integrated EU/FP6 project and one of the major projects of the International Polar Year (IPY: March 2007 - March 2009), which aims at observing, understanding and quantifying climate changes in the Arctic. One of the objectives of DAMOCLES-IP is to develop and test new ocean and sea ice technologies and contribute to the development of a future Arctic Ocean Observation System. In this framework a tomography experiment will be conducted from September 2008 to September 2009 to monitor the average heat content across the Fram Strait and contribute to improved estimation of heat fluxes through the strait by assimilation of tomography data in fine-scale oceanographic models [1,2].

The deep and wide Fram Strait, between Greenland and Spitzbergen, is the main passage through which the mass and heat exchange between the Atlantic and Arctic Ocean takes place: on the eastern side of the strait the northward West Spitzbergen Current (WSC) brings Atlantic water to the Arctic Ocean whereas on the western side the southward East Greenland Current (EGC) brings cold water from the Arctic back to the Atlantic ocean. Between these two current systems the Return Atlantic Current (RAC) recirculates water masses from the western flank of the WSC back into the Atlantic (see Fig. 1). The RAC is responsible to a large extent for the variability in the heat flux through the strait [3].
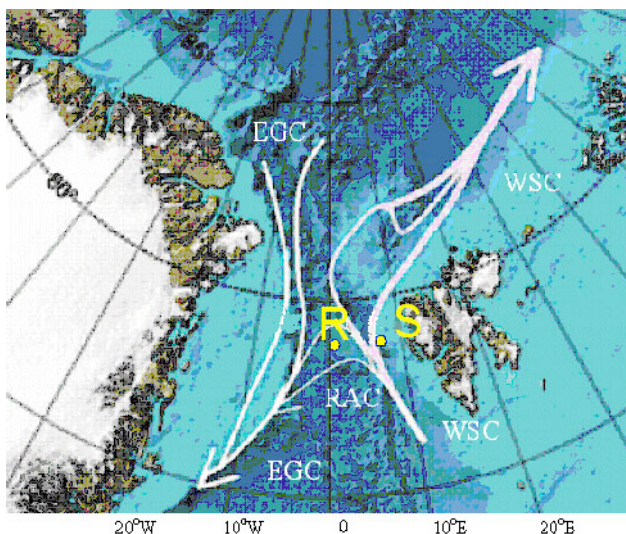

Fig.1   Experiment setup

The design of the tomography experiment sought to maximize the information content of the acoustic receptions

taking into account the propagation characteristics as well as the particular features of the selected instruments. Both source and receiver moorings will be deployed near the latitude of 78°50′N, to take advantage of an existing array of in situ measurements at this latitude [3]. Fig.1 shows the location of the moorings at the experiment site. The source will be placed at 7°E and at a depth of 400 m. The receiver mooring will be placed at 1°E with 8 hydrophones at depths between 300 and 1000 m. The corresponding section (propagation range of 129.7 km) covers the WSC and the RAC to a significant extent.

The tomographic travel-time data collected from the experiment site will be transmitted through the internet to a dedicated server for further analysis. A software system called SMTAS (Streaming Mode Tomographic Analysis System) has been developed to manage the overall data transmission and processing operation.

2   Travel time inversion scheme

Tomographic data, in the form of travel-times corrected for clock drift and mooring motion effects, will be analyzed using the matched-peak (MPT) inversion approach [4,5]. This approach consists in finding the population of model states that identify the maximum number of peaks in each reception. For this purpose the parameter domain is discretized into a finite set of model states. Using the model relations, arrival times are predicted for each model state and compared with the observed ones seeking to maximize the number of identifiable peaks. The matched-peak approach offers a weak solution to the identification problem (association between theoretical and observed peaks) and thus by-passes the uncertainties associated with the explicit solution of this problem.

To apply the matched-peak approach, the temperature distribution is parameterized using empirical orthogonal functions (EOFs) obtained from principal-component analysis of 3-year long (2002 - 2005) time series of temperature from the moored ASOF array [3].
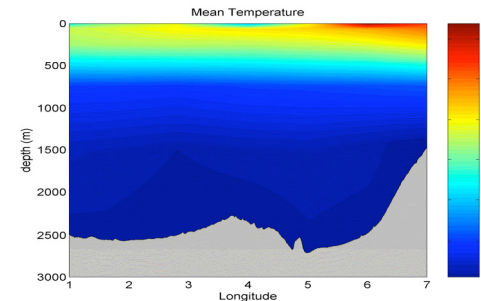

Fig.2   Mean temperature distribution from the ASOF data

The Chen-Millero formula is used to convert temperature distributions into sound-speed distributions assuming a constant salinity of 35 ppt, which is an average value for the salinity in the area of interest [6].

The effects of range dependence on travel-times are taken into account in the model relations by using a range dependent background ocean state and range dependent EOFs. Fig. 2 shows the 3-year average temperature distribution from the ASOF data along the 78°50′N section between 1°E and 7°E. The basic thermocline at 500 m depth and the warm-water signature of the West Spitzbergen current on the east are seen in this figure. Fig. 3 shows the first four temperature EOFs for the same section as functions of range and depth.
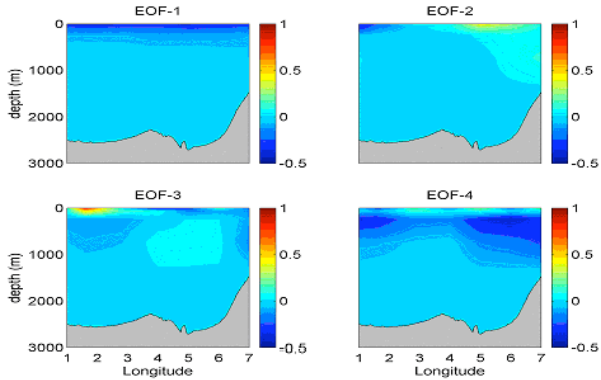

Fig.3   The first four temperature EOFs based on the ASOF data

The rms amplitudes for the first ten EOFs are shown in Table 1. The first five EOFs explain 92%, the first ten 97.8% of the variability of the ASOF data.

EOF order ℓ	RMS amplitude $\vartheta_{\ell,\mathrm{rms}}$	EOF order ℓ	RMS amplitude $\vartheta_{\ell,\mathrm{rms}}$
1	3.4866	6	0.5346
2	1.0878	7	0.502
3	0.9421	8	0.3986
4	0.8118	9	0.3775
5	0.6859	10	0.3541

Table 1: Rms amplitudes for the first ten EOFs

3   Synthetic tomography experiment

The efficiency of the inversion method is assessed using synthetic travel-time data produced from the 3-year long time series of the EOF amplitudes corresponding to the ASOF data. Fig. 4 shows the time series of the first five EOF amplitudes over the 3 years of the ASOF data. A clear seasonal signal can be observed in the evolution of the EOF-1 amplitude, whereas there is no apparent such signal in the amplitudes of the higher-order EOFs. This indicates that the first EOF, which is the most significant one (s. Table 1), accounts for the bulk of the seasonal variability,

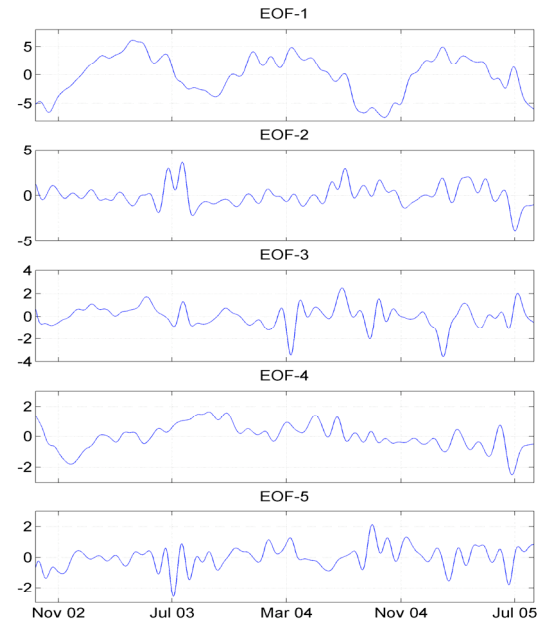whereas the remaining EOFs describe modes of temperature change due to mesoscale variability.

Fig.4   The evolution of amplitudes of the first five EOFs in the ASOF data from summer 2002 to summer 2005.

For each day the first ten EOFs are used to generate a range-dependent temperature and sound-speed distribution. Then a ray-tracing code is applied to predict arrival patterns and travel times at the 8 hydrophone depths (from 300 to 1000m with a step of 100 m). Travel-times closer than 10ms, are grouped and replaced by their average. The resulting synthetic travel-time data for the depth of 900m are shown in Fig. 5. The seasonal variability observed in the evolution of the EOF_1 amplitude in Fig. 4 reflects in the overall travel-times in Fig. 5 (earlier arrivals in summer than in winter), with an exception in summer 2003 during which the seasonal warming signal is weak. Further, the warming of the near surface layers in summer increases the sound-speed variability in the vertical and leads to increased time spread of the arrival pattern.
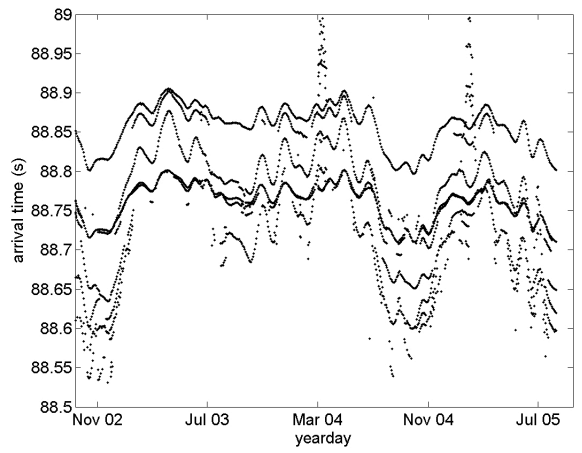

Fig.5 The evolution of synthetic travel times for the depth of 900m

The implementation of model relations required for each inversion relies on travel-time calculations. These calculations are carried out for a grid of discrete model states and the results are stored in a database so that they can be used for subsequent inversions. The structural design of this database supports dynamic adaptation to changes of either the number of the contained EOFs or the number of discrete amplitude values of any particular EOF. The first five EOFs are used for the inversions, with their amplitudes discretized as indicated in Table 2. The maximum / minimum values of the discretization intervals are taken ±2-3 times the corresponding rms values (Table 1) to span the anticipated variability.

EOF order	Amplitude discretization
1	-7: 0.5: 7 (29 values)
2	-4: 1: 4 (9 values)
3	-3: 1: 3 (7 values)
4	-2: 1: 2 (5 values)
5	-2: 1: 2 (5 values)

Table 2: Amplitude discretization for the first five EOFs

Fig. 6 shows the time-depth plot at the receiver for the date of 31 October 2004. The dots on this figure correspond to the synthetic travel-time data whereas the lines represent the predicted time-depth dependence corresponding to a member of the population of model states selected by the matched peak approach. It is seen that a good representation of the synthetic data is obtained.
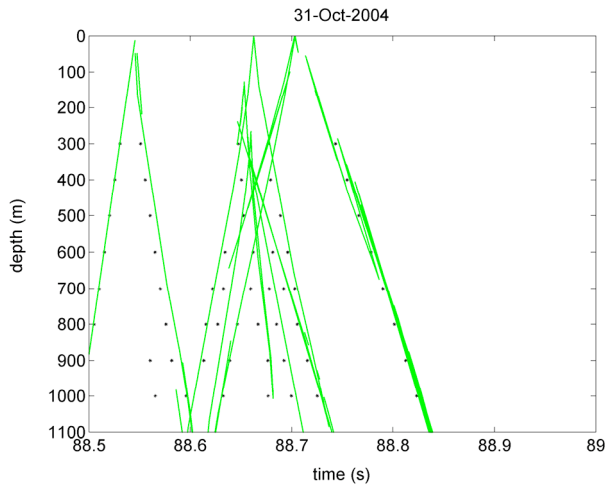

Fig. 6 Time-depth plot at the receiver on 31 October 2004. Black dots: synthetic data at the 8 hydrophone depths. Green lines: Time-depth predictions corresponding to one member of the population of selected model states.

Fig. 7 presents the inversion results in the form of range-averaged temperatures at the ASOF depths: 50, 250, 750, 1500 and 2500 m. The red dots represent the original temperatures. The population of green dots represents the population of selected model states in each inversion, whereas the heavier blue dot is the mean out of this population of temperatures. A good agreement between the original and the recovered temperatures is obtained as far as the mean temperatures are concerned. The spread of the temperature populations (green dots) describes the uncertainty of the obtained mean values.
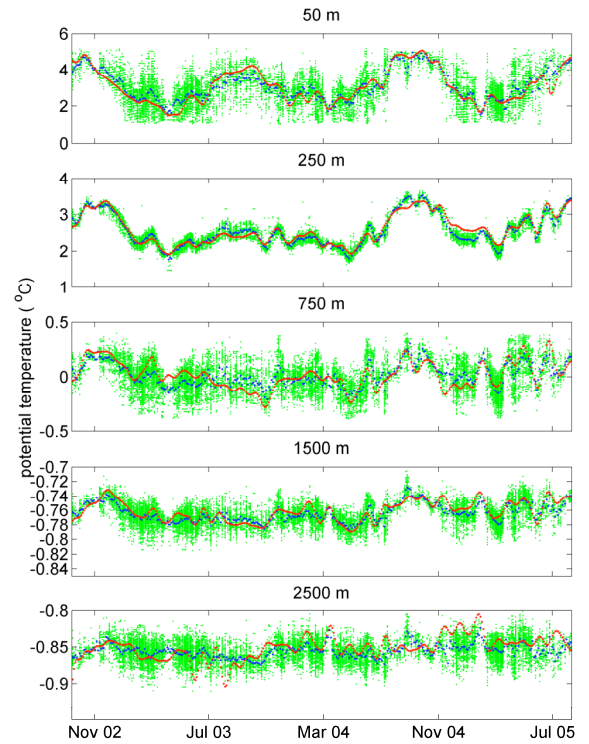

Fig.7 Evolution of range-averaged temperature at the ASOF depths - comparison between original temperatures (in red) and inversion results (in green, blue).

From this figure it is seen that the uncertainties are different from depth to depth and from season to season. Indeed, the inversion results at 250m (and to some extent at 1500m) depth have smaller uncertainties compared to the remaining layers. Further, the inversion errors are in general smaller when the temperatures are higher e.g. in summer 2004.

A physical explanation for the different errors at different layers is that having the source placed at 400m, the depth of 250 m is turning depth to a large number of rays. The same applies to a lesser extent for the depth of 1500 m. On the other hand the depth of 750 m lies close to the deep axis (minimum sound-speed) such that the grazing angles at 750m are close to maximum. The travel-time sensitivity of rays is known to become largest at the turning depths and smallest at the depths of maximum grazing angles (layers where the rays spent the shortest time) [7]. This higher sensitivity explains the smaller inversion errors at 250 and 1500 m compared to 750 m.

The smaller errors in the high temperature seasons can be explained by the fact that rays are surface reflected in winter and refracted in summer, when the temperatures close to the surface are high. This means that in summer they have turning depths close to the surface, i.e. spend longer times close to the surface. In winter they have larger grazing angles and spend shorter times close to the surface. This leads to a higher sensitivity (smaller inversion errors) when the near-surface temperatures rise. This is clearly seen in the inversion results for the 50m depth.

4 Streaming Mode Tomography Analysis System (SMTAS)

Tomographic travel-time data from the experiment will be transmitted for further processing and analysis to a dedicated server running an integrated software called SMTAS (Streaming Mode Tomographic Analysis System). SMTAS allows for both on-line (near-real-time) analysis of incoming data and off-line (batch mode) analysis of already stored data.
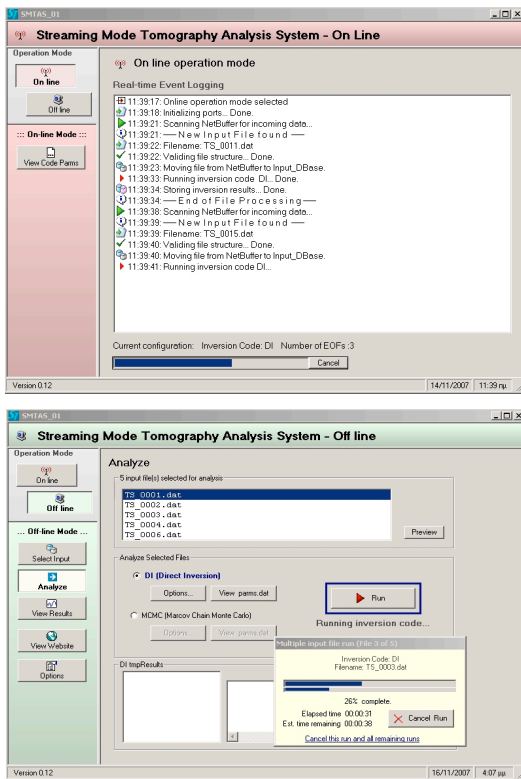

Fig.8 Sample screenshots of the SMTAS during a) on-line and b) off-line operation.

SMTAS supports asynchronous reception, validation, processing and inversion of acoustic tomography data. The data will be transmitted directly from the experiment location or sent in batches at a later time, whenever data are manually recovered from the moorings. A first level of preprocessing will be carried out inside the tomography instruments such that the transmitted data are free of clock-drift errors and mooring-motion effects. All dataflow is performed in near-real time through the internet using standard communication protocols (SMTP and POP3).

The inversion results produced by SMTAS, in the form of horizontally averaged temperature profiles or heat contents of particular depth layers and associated error estimates, are archived locally. A selected fraction of the results is uploaded in near-real time to a web site for further dissemination. To assess the functionality of SMTAS, a number of simulated data transmissions have been performed using synthetic data. The system was then used to receive, validate, process, archive and disseminate the produced inversion results in near-real time. Figure 8 displays two sample screenshots of SMTAS during on-line and off-line operation.

5 Conclusions

In this work a first assessment of the inversion method for the Fram Strait tomography experiment is carried out using synthetic travel-time data. While the inversion results for the mean temperatures are well comparable with the original temperatures, the inversion errors exhibit spatial and seasonal dependence. In particular, there are layers, e.g. around 250m depth, where the inversion errors are smaller pointing to a higher sensitivity of travel-times to sound speed changes at those depths. Further inversion errors are expected to be smaller during periods where the temperatures close to the surface are high, i.e. in general smaller in summer than in winter.

Acknowledgments

References

[1] Evensen G., "The Ensemble Kalman Filter: theoretical formulation and practical implementation", *Ocean Dynamics* 53, 343-367 (2003).

[2] Bertino L., K.A. Lisæter, H. Sagen, *et al*. "Towards an Operational Prediction system for the North Atlantic and European coastal Zones" TOPAZ final report, *NERSC Technical Report* 251 (2004).

[3] Schauer, U., Beszczynska-Möller, A., Walczowski, W., Fahrbach, E., Piechura, J., Hansen, E., "Variation of Measured Heat Flow Through the Fram Strait Between 1997 and 2006", in *Arctic-Subarctic Ocean Fluxes: Defining the Role of the Northern Seas in Climate*, R.R. Dickson et al. Eds., Springer B.V., 65-85. (2008).

[4] E.K. Skarsoulis, "A matched-peak inversion approach for ocean acoustic travel-time tomography", *Journal of the Acoustical Society of America* 107, 1324-1332 (2000).

[5] E.K. Skarsoulis, U. Send, G. Piperakis, P. Testor, "Acoustic thermometry of the western Mediterranean basin", *Journal of the Acoustical Society of America* 116, 790- 798 (2004).

[6] Beszczynska-Möller A., Fahrbach E., Schauer, U., Rohardt E., Wisotzki A., "Arctic-Subarctic Ocean Flux Array for European Climate: Preliminary data from moored array and repeated sections" *ASOF_N D3.2 Report* (2004)

[7] Cornuelle, B. D., P. F. Worcester, J. A. Hildebrand, W. S. Hodgkiss Jr., T. F. Duda, J. Boyd, B. M. Howe, J. A. Mercer and R. C. Spindel, "Ocean acoustic tomography at 1000-km range using wavefronts measured with a large aperture vertical array", *J. Geophys. Res* 98, 16365-16377 (1993).